

# A review of the gas diffusion layer in proton exchange membrane fuel cells: Durability and degradation



Jaeman Park<sup>a</sup>, Hwanyeong Oh<sup>a</sup>, Taehun Ha<sup>b</sup>, Yoo Il Lee<sup>a</sup>, Kyoungdoug Min<sup>a,\*</sup>

<sup>a</sup> Department of Mechanical and Aerospace Engineering, Seoul National University, 1 Gwanak-ro, Gwanak-gu, Seoul 151-744, Republic of Korea

<sup>b</sup> Advanced Institutes of Convergence Technology, 145 Gwanggyo-ro, Yeongtong-gu, Suwon-si, Gyeonggi-do 443-270, Republic of Korea

## HIGHLIGHTS

- This paper focuses on the evaluation of the durability characteristics of GDL.
- GDL degradation can be categorized into mechanical and chemical degradation.
- Standardized test protocols need to be established to evaluate GDL durability.

## ARTICLE INFO

### Article history:

Received 11 May 2015

Received in revised form 17 June 2015

Accepted 23 June 2015

Available online 6 July 2015

### Keywords:

Proton exchange membrane fuel cell

Gas diffusion layer

Durability

Degradation mechanism

## ABSTRACT

For successful commercialization of a proton exchange membrane fuel cell, the durability requirement must be satisfied. The degradation of a proton exchange membrane fuel cell has been extensively studied, and a number of review papers investigating the durability issue have already been published. However, the gas diffusion layer has rarely been examined, even though it might be a key factor for managing mass transport and two-phase flow while mechanically supporting a membrane-electrode assembly and a bipolar plate. This paper reviews the published works on the durability of the gas diffusion layer of the proton exchange membrane fuel cell. The degradation of the gas diffusion layer can be divided into mechanical degradation, including the compression force effect, freeze/thaw cycle effect, dissolution effect, and erosion effect, and chemical degradation, which consists of the carbon corrosion effect. Following these categories, the methods of accelerated stress tests, the degradation mechanisms, and the influential factors are investigated along with various measurements of gas diffusion layer properties and cell performances.

© 2015 Elsevier Ltd. All rights reserved.

## Contents

1. Introduction .....	866
2. GDL degradation process .....	867
3. Mechanical degradation on GDL .....	868
3.1. Effect of compression force .....	868
3.2. GDL degradation under freezing/thawing condition .....	870
3.3. Dissolution effect on GDL .....	872
3.4. Erosion of GDL by continuous gas flow .....	873
4. Chemical degradation on GDL .....	874
4.1. Carbon corrosion phenomena of GDL .....	874
5. Summary .....	878
Acknowledgments .....	878
Appendix A .....	878
References .....	878

\* Corresponding author. Tel.: +82 2 880 1661; fax: +82 2 883 0179.

E-mail address: [kadmin@snu.ac.kr](mailto:kadmin@snu.ac.kr) (K. Min).

## 1. Introduction

Global warming, caused by increasing concentrations of greenhouse gases, is one of the largest environmental issues of the 21st century [1–4]. Specifically, approximately 17% of carbon dioxide emissions comes from the burning of petroleum in the internal combustion engines of cars and trucks [5]. Therefore, reducing the dependence on oil in transportation is one solution to avoid environmental disaster. Proton exchange membrane (PEM) fuel cell technology has received significant attention as a potential alternative source of power generation for automotive applications in terms of zero-emission, high efficiency, and quick response to load changes. However, durability concerns must be resolved before PEM fuel cell technology can be deployed on a commercial scale; hence, PEM fuel cell durability has attracted enormous research and development (R&D) attention during the last decade.

The central part of the fuel cell system is the membrane-electrode assembly (MEA), consisting of a proton conducting membrane with anode and cathode catalyst layers. The membranes need to be hydrated to maintain high proton conductivity and ensure adequate fuel cell performance. However, excess water in the electrodes can result in electrode flooding, which prevents electrochemical reactions from occurring and reduces performance, thus a careful balance must be maintained [6–17]. In this respect, the gas diffusion layer (GDL) which is in contact with catalyst layer is one of the critical components of a fuel cell that has the ability to influence the system performance because its basic functions are transporting the reactant gas from the flow channel to the catalyst layer, draining liquid water from the catalyst layer to the flow channel, conducting electrons with low resistance, and keeping the membrane in a wet condition at low humidity. Although there are various types of GDLs and new structural concepts are being developed, the GDL is typically made of carbon fibers and consists of a macro-porous substrate and a micro-porous layer (MPL), as presented in Fig. 1. The substrate, in contact with the gas flow channel, serves as a gas distributor and a current collector. The MPL contains carbon powder and hydrophobic agent and also manages the two-phase water flow. However, due to the durability of the material characteristics of the GDL, the core abilities of the GDL such as hydrophobicity, conductivity, and mechanical strength are reduced during operation. Therefore, a large amount of R&D has been carried out by universities, research institutes and commercial organizations to determine the durability characteristics of GDLs independently [18–22].

Many reviews of MEA durability have been published [23–39] and can be summarized as the durability of MEA is largely influenced by the degradation of catalyst and carbon supports. As

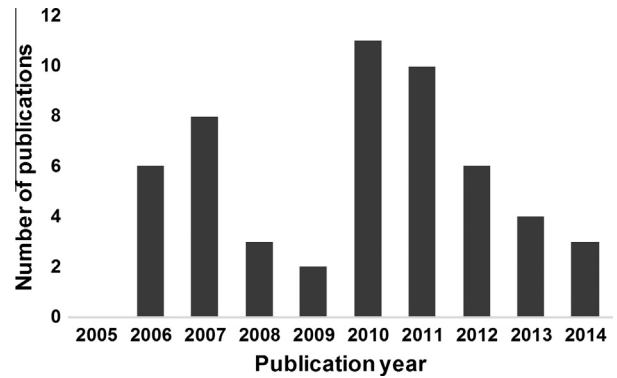


Fig. 2. Bibliometric analysis of the publications.

MEA degrades, platinum particles agglomerate, which reduces the active surface area, and consequently leads to performance deterioration. In particular, the durability of MEA is highly dependent on cell potential, humidity, temperature, contaminants of supply gases, and carbon support stability. However, the durability research summaries on GDL degradation are relatively limited, while its importance is highlighted.

In this paper, review of GDL degradation was conducted by categorizing several degradation methods. Variations of the GDL material properties according to GDL degradation and the effect of GDL degradation on PEM fuel cell performance are summarized. A bibliometric analysis of the publications on the degradation or durability of GDL since 1999 has been carried out. The data were found using the Science Citation Index (SCI), Web of Science. According to Journal Citation Reports (JCR) [40], it indexed 10,927 journals in 237 scientific disciplines in 2014. “Gas diffusion layer” and “degradation” or “durability” were used to search titles, abstracts, or keywords. In addition, several theses and book chapters are included in this paper. The number of publications over the past 10 years (Fig. 2) reveals that the degradation and durability research on GDLs have received considerable attention within the area of fuel cell research.

## 2. GDL degradation process

Understanding the GDL degradation process is required to investigate the GDL durability problems, but the degradation occurs through highly complex reasons and processes. Hence, separating out each of the reasons and investigating the effects of each individual are important.

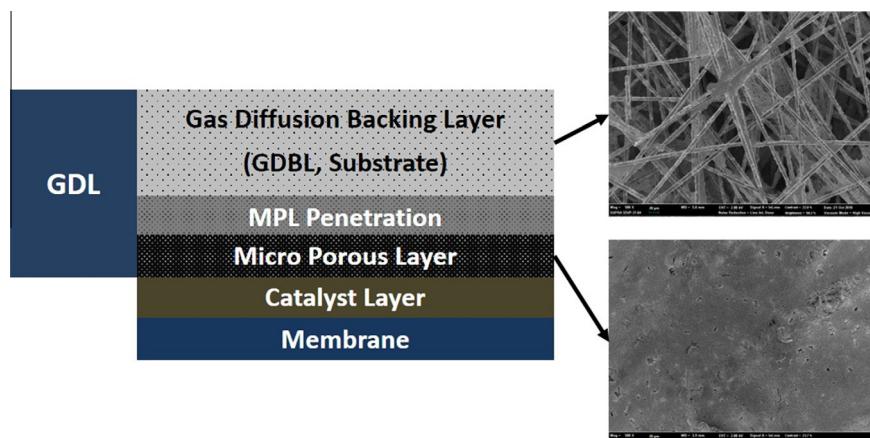


Fig. 1. A schematic diagram of the GDL structure.

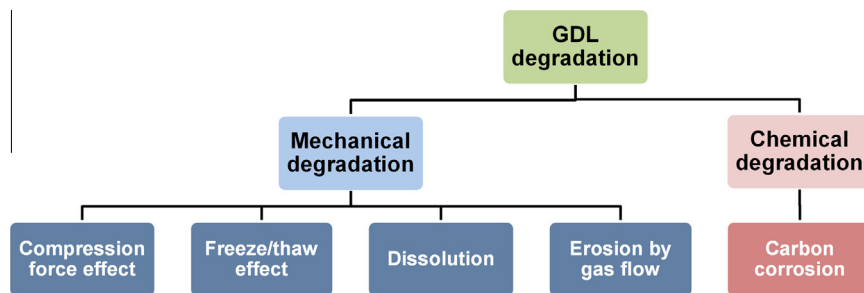


Fig. 3. Degradation mechanisms of the GDL.

GDL degradation can be categorized into mechanical and chemical degradation, as presented in Fig. 3. The mechanical degradation is literally physical damage and consists of mechanical breakdown by compression, freezing/thawing, dissolution in water, and erosion by gas flow. GDL is the most compressible structure among the fuel cell components, and it therefore absorbs most of the clamping force and suffers structural damage. The PEM fuel cell of automotive applications experiences a freezing/thawing cycle. In addition, externally supplied water through humidifier and electrochemically produced water gradually dissolves the GDL. Continuously supplied gas flow also causes mechanical degradation of the GDL. The chemical degradation is mainly due to carbon corrosion. The GDL is made of carbon, and at some special conditions such as start-up, shut-down or local fuel starvation, the carbon reacts with the water and is washed away, causing structural breakdown.

This paper focuses on the review of the in-situ and ex-situ experiments used for evaluating the durability characteristics of GDL, as well as the results and analyses along with recent developments and future directions. The GDL degradation related papers are categorized and analyzed in the following order. Firstly, the compression effect of mechanical degradation is reviewed. Compression is related not only to mass transport and electric conductivity but also to a geometric shape change of the GDL. Secondly, the freeze/thaw effect of mechanical degradation is addressed. Thirdly, the dissolution effect of water is presented. These degradation factors are closely related to the electric conductivity and hydrophobicity. Fourthly, the sole erosion effect on GDL by the gas flow is discussed. Finally, the carbon corrosion effect of electrochemical degradation, which affects the GDL capability of water discharge, is given and followed by a summary. Table 1 presents a classification of the durability tests of GDL in the literature.

### 3. Mechanical degradation on GDL

#### 3.1. Effect of compression force

Most PEM fuel cells consist of channel-machined bipolar plates, GDLs and MEAs where electrochemical reactions take place. The MEA is the center, with the GDLs and then the bipolar plates placed on either side. All of these components are held together with high compression to prevent gas leakages and provide low contact resistances as well. The compression pressure strongly affects the properties of the GDL, the GDL/catalyst layer interface, and the bipolar plate interface, and these changes consequently influence the overall cell performance. As the compression pressure increases, the overall pore volume and gas permeability of the GDL decreases, resulting in higher mass transport overpotential. At the same time, compressing the GDL improves the contacts between its fibers and with other components. These better contacts enhance its electric and thermal conductivity, and, as an outcome, the ohmic overpotential is decreased. In other words, compressing the GDL influences both the mass transport overpotential and the ohmic overpotential, but they indicate a counter-trend. The effect of compression on the GDL characteristics and degradation has been elucidated by various researchers. Fig. 4 shows the degradation mechanisms of the GDL and the effects on a fuel cell of increased compression force [41].

As mentioned previously, increasing the compression of the GDL affects the GDL permeability. The results of Chang et al.'s work [42] showed that when the carbon paper was compressed to half of the total thickness, the permeability decreased to one-tenth of the initial permeability value. Nitta et al. [41] also confirmed that the GDL permeability decreased as much as one order of magnitude when the GDL was compressed to 65% of the initial thickness. In addition, the degree of the permeability decrease in the GDL varies

Table 1

Classification of the GDL durability tests in the literature.

Degradation condition	Approaches	Ref.
Compression force	Single compression Repetitive compression	[41–51,53,54] [52,55]
Freeze/thaw	Cold start Temperature cycling	[19,64,72,73] [20,56–63,65–67,70,71]
Dissolution	Immersion in solutions Long-term operation	[74,76,79,81–83] [75]
Erosion by gas flow	Exposure to excessive gas flow	[22,85]
Carbon corrosion	Three-electrode test Potential holding Potential cycling Potential holding and cycling	[87,89,95] [88,92–94] [97,98] [96]
Compression force and carbon corrosion	Repetitive compression and three-electrode test	[90]
Dissolution and erosion by gas flow	Immersion in solutions and exposure to excessive gas flow	[78]
Dissolution and carbon corrosion	Immersion in solutions and potential holding Immersion in solutions and potential cycling	[77,80,91] [84]

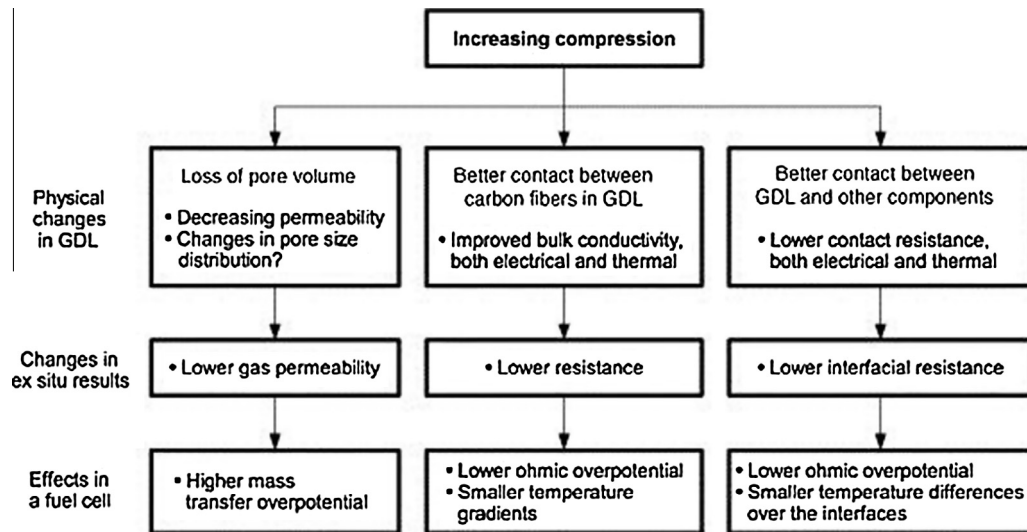


Fig. 4. Effects of increasing compression of the GDL. (From [41] with permission.)

with GDL types. Ihonen et al. [43] found that the decrease in permeability of the carbon cloth-type GDL is the most severe under increasing clamping pressure because it has the least rigid mechanical structure.

Although compressing the GDL has a negative effect on the gas permeability, compression decreases the through-plane electrical resistance and the electrical contact resistance between GDL and other components. Chang et al. [42] reported that the electrical contact resistance was substantially decreased from  $1000 \text{ m}\Omega \text{ cm}^2$  at the initial state to  $180 \text{ m}\Omega \text{ cm}^2$  at an external clamping pressure of 2.5 bars and then eventually reached a steady-state value as the clamping pressure increased beyond 2.5 bars. They also discovered that the through-plane resistance decreased with increasing clamping pressure, but it was insignificant compared to the electrical contact resistance. According to Nitta et al. [41], the compression has a remarkable effect on the bulk GDL conductivity because the decrease in thickness reduces the distances between the conductive carbon fibers, which improves contact among the fibers. As a result, the contact resistance of the GDL changed significantly with the compression pressure. In addition, the contact resistance between graphite and GDL was varied up to one order of magnitude as the GDL with an original thickness of  $380 \mu\text{m}$  was compressed to  $350$  or  $250 \mu\text{m}$ . Mishra et al. [44] measured the contact resistances of various paper-based and cloth-based GDLs according to the clamping pressures. They found that when the clamping pressure was less than 1.5 MPa, the contact resistance of the GDL with MPL was measured to be higher than that without MPL. Conversely, for pressures over 1.5 MPa, the contact resistance of the GDL without MPL was higher than that with MPL.

The trade-off relationship between the GDL compression effect on the mass transport and the ohmic overpotential have opposite effects on the cell performance. Chang et al. [42] reported a negligible difference in the performance curve under GDL compression from 10 to 20 bars. However, the polarization curve displayed an improvement in the maximum limiting current density with enhanced mass transfer behavior under compression pressure up to 10 bars. Yim et al. [45] investigated the effect of GDL compression on performance in a five-cell PEM fuel cell stack. They observed that a high GDL compression (30% compression in thickness) enhanced the stack performance compared to low GDL compression (15% compression in thickness) at all current ranges. These results mean that the decrease in stack performance from

contact resistance under high compression is more dominant than the effect of an increase in mass transport resistance. From these previous results, it can be concluded that there is an optimum compression ratio for each PEM fuel cell environment.

Several papers investigate the effect of compression according to different types of GDLs [46–50]. Lee et al. [46] conducted an experiment of PEM fuel cell performance under different bolting torques and found that there is an optimum bolting torque for each type of GDL. Ge et al. [47] researched the effect of GDL compression on PEM fuel cell performance under a number of different operating conditions with a variety of GDL types. In their paper, the paper-type GDL exhibits the greatest compression effect, especially in the high current density region. They concluded that the cell performance is maximized with an optimal GDL compression ratio. Lin et al. [48] found that there is an optimum compression ratio for each GDL using two different types of GDL.

Several studies have addressed the durability of GDL under compression. In some papers, the structural changes within the GDL were observed. Matsuura et al. [51] found that negligible damage appeared on the GDL when its compressive displacement was  $20 \mu\text{m}$ . However, the breakage of carbon fibers in the GDL was observed at a compressive displacement of  $120 \mu\text{m}$ , as shown in Fig. 5. Radhakrishnan et al. [52] conducted the experiment of 5-cyclic compression of GDL at two different compression pressures (1.7 MPa and 3.4 MPa). They observed both surface and cross-sectional morphologies. The GDL samples started to suffer from fiber breakage and showed cracks at the third cycle, and considerable damage occurred in the GDL at both 1.7 MPa and 3.4 MPa after five cycles. They also measured the GDL surface roughness using a laser profilometer and found that under a cycle of compression, the sample showed a gradual decrease in surface roughness. Bazylak et al. [53] observed the scanning electron microscope (SEM) images of the GDLs after they were compressed for five minutes at a pressure of 0.18, 0.36, 0.68, and 1.37 MPa. The images showed breakage of polytetrafluoroethylene (PTFE) coatings or detachment of PTFE from the carbon fibers. As the compression pressure increased, the amount of damage also increased. The results of Lin et al.'s [48] research showed that the GDL with high bulk density (i.e., more carbon fibers per unit volume) dispersed the compressive force so that a more uniform force was applied to the GDL, and as a result, damage to the carbon fibers could be mitigated. The structural change and/or the loss of PTFE affects the hydrophobicity of the GDL. Radhakrishnan et al. [52] reported



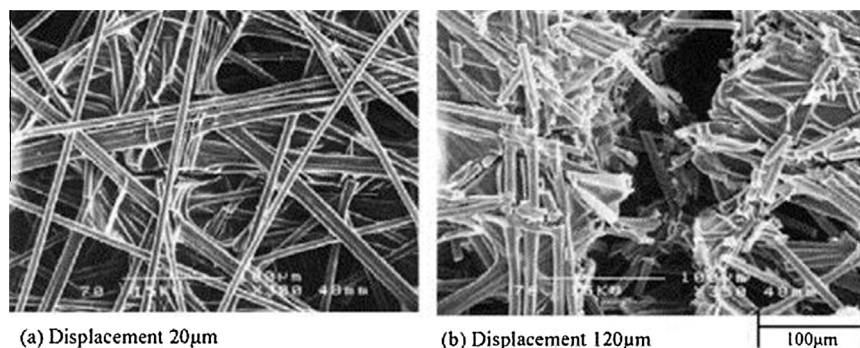


Fig. 5. SEM images of GDL carbon fibers after GDL compression: (a) for compressive displacement of 20  $\mu\text{m}$  and (b) 120  $\mu\text{m}$ . (From [51] with permission.)

that the contact angle of the GDL decreased when cyclic compression was applied to the GDL. Bazylak et al. [53] also showed that the loss of PTFE creates localized hydrophilic routes that became preferable pathways for the transport of water in the GDL. The loss of PTFE content in the GDL can be minimized by increasing the number of PTFE treatments on the GDL. Kumar et al. [54] found that the GDL with single PTFE treatment showed an approximately 23% decrease in the contact angle after five compression cycles, and this decreased to 12% and 9% by increasing the number of PTFE loading to three and six stages, respectively.

Performance degradation occurs due not only to the GDL but also to the membrane under GDL compression conditions. Matsuura et al. [51] observed the change in open-circuit voltage (OCV) over time using the cell with a compressive displacement of 20 and 100  $\mu\text{m}$ . The GDL with a compressive displacement of 100  $\mu\text{m}$  showed a significant decrease in the OCV during the very early phase. These researchers concluded that the reason for the decrease in the OCV was damage to the electrolyte membrane, which causes a short-circuiting of the membrane or a crossover of reactant gas, such as hydrogen. However, the researchers did not elucidate how the membrane was damaged during the compression. Baik et al. [55] studied the effects of the GDL structure on OCV and hydrogen crossover. They used three types of commercial GDL: (1) carbon fiber felt substrate with rough surface MPL, (2) carbon fiber felt substrate with smooth surface MPL, and (3) carbon fiber paper substrate with smooth surface MPL. These different types of GDLs were compressed under various clamping torque values, and the results showed that the tendency of hydrogen crossover in each GDL is similar to that of OCV. The carbon felt GDL with rough surface MPL showed the highest hydrogen crossover rate and OCV reduction as the clamping torque increased. They concluded that hydrogen crossover resulted from the puncture of the membrane by the GDL. As a result, this damage reduces the OCV and affects the membrane degradation behavior.

### 3.2. GDL degradation under freezing/thawing condition

For an automotive application, a PEM fuel cell is exposed to sub-freezing temperatures, especially in the winter season. When the temperature of a PEM fuel cell dips under the freezing point of water, any residual water left after shutdown or water generated during a cold start process is likely to be frozen. During the phase change, sizeable volumetric expansion occurs and causes mechanical stress on cell components such as membranes, catalyst layers and GDLs. Among the various cell components, the degradation of the MEA has been steadily shown during a freeze/thaw process. The various MEA degradation mechanisms were investigated and can be summarized as follows: the formation of a crack or cavity, frost heave, void formation, the loss of platinum from a catalyst layer, the delamination of a catalyst layer from a membrane, the

decrease in the electrochemical active area, and the increase in the contact resistance near the MEA [56–63]. Meanwhile, only a handful of papers focus on GDL degradation, regardless of the fact that a GDL is also an important factor in how quickly a PEM fuel cell degrades because it controls the water content in the GDL and its surrounding components, such as the membrane and catalyst. The GDL can also affect the mechanical resistance as a physical supporter, distributing the compressive pressure generated during the freeze/thaw process.

In the early stages, studies were focused only on how GDLs degrade. Yan et al. [64] reported that the GDL surface became rough as the PTFE coating and binder structure were damaged by ice formation when the cell starts to operate below  $-15^\circ\text{C}$ . This phenomenon is likely to decrease the gas permeability and increase the electronic conductivity. However, Lee et al. [20] found no effects on the strain, the in-plane electrical resistivity, the bending stiffness, the surface contact angle, the porosity, or the water vapor diffusion, except for the increase in the in-plane and through-plane air permeability, after the process of 54 freeze/thaw cycles between  $-35^\circ\text{C}$  and  $20^\circ\text{C}$  with a test fixture under fully saturated conditions.

Since then, not only the degradation mechanism but also the factors of the GDL that can affect the PEM fuel cell durability have been studied. The most influential property of the GDL that affects the PEM fuel cell durability is the stiffness. A GDL with high stiffness can distribute the compressive force more evenly on ribs and ease the volumetric deformation caused by ice formation [62,65,66]. Generally, a felt-type GDL has a higher stiffness than a paper-type due to the more rigid shape of the three-dimensional structure, unlike the two-dimensional structure of the paper-type. Mukundan et al. [19,67] investigated the effect of freezing water by comparing the paper-type GDL to the cloth-type GDL. They measured the cell performance and the electrochemical impedance spectroscopy (EIS) data of both GDLs that underwent repetitive freezing temperatures of  $-40^\circ\text{C}$ . The authors discovered that the mass transport loss increases more severely with the paper-type GDL and that the ice formation intensively occurs in the cathode catalyst layer/GDL near channel inlets and outlets with neutron images. In addition to the change in cell performance, the structural changes of the cell components according to GDL types has been shown. Lim et al. [65] confirmed that the felt-type GDL, which has the highest bending stiffness among other GDLs, offers more stable performance than the paper-type or cloth-type GDLs. Because the felt-type GDL possesses the smallest gap between the GDL and MEA, it shows the smallest alteration of the MEA surface under the channel and the smallest increase in the ohmic resistance (Fig. 6) during the freeze/thaw process of  $-30^\circ\text{C}$  to  $70^\circ\text{C}$ . In addition, Kim et al. [56,62] compared the effect of the felt-type GDL to the paper-type GDL, focusing on the physical damage of the MEA during a freeze/thaw cycle process from  $-40^\circ\text{C}$  to  $70^\circ\text{C}$ . It was analogized that the uniformity of

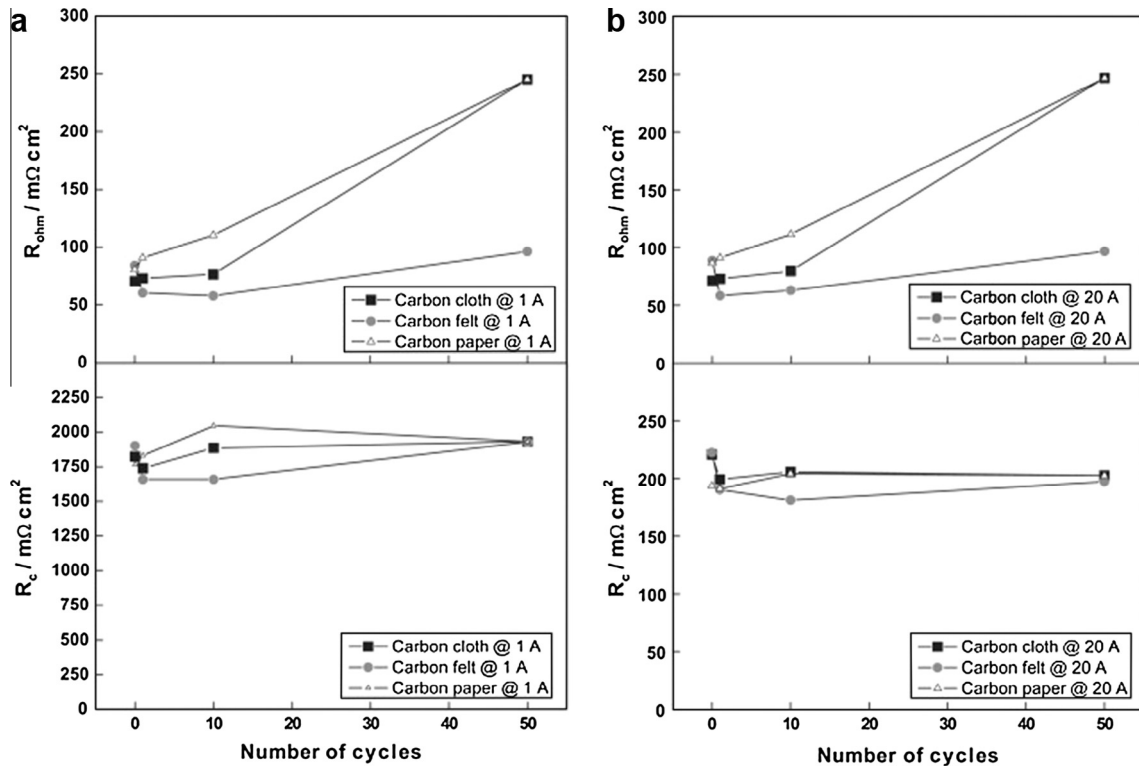


Fig. 6. Changes in resistance of cells under freeze/thaw cycles according to the GDL types at the current of (a) 20 mA/cm<sup>2</sup> and (b) 400 mA/cm<sup>2</sup>. (From [65] with permission.)

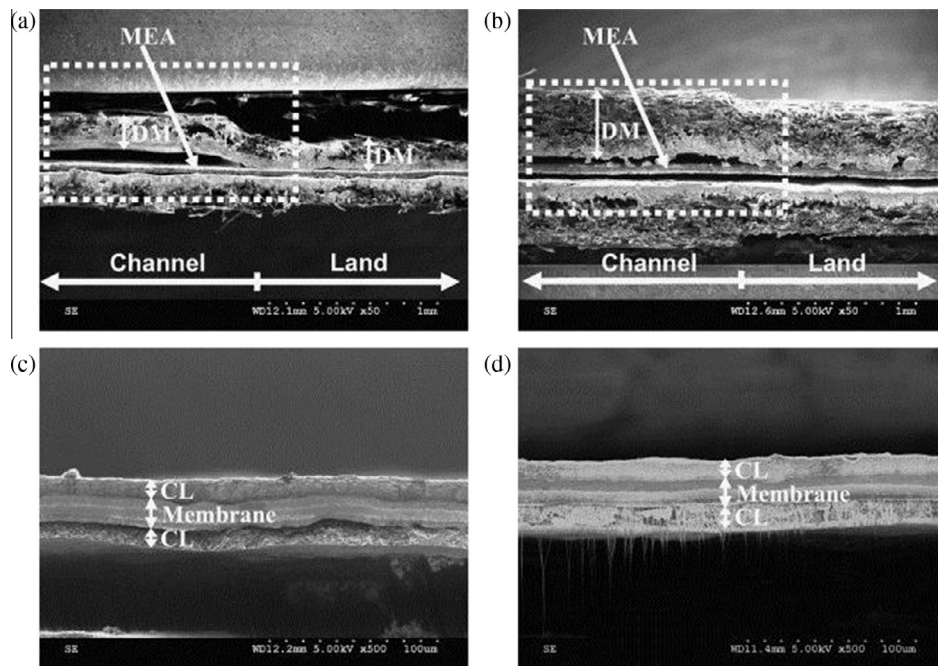


Fig. 7. Cross-sectional images of MEA and diffusion media after 100 freeze/thaw cycles: (a) and (c) SGL 25BC (paper-type); (b) and (d) SGL 10BB (felt-type). (From [62] with permission.)

compressive pressure with higher stiffness on a catalyst layer can be a key factor in mitigating physical damage such as interfacial delamination or frost heave between the diffusion media and a catalyst layer. This can be observed through SEM and high frequency resistance (HFR), as shown in Fig. 7. Another factor that affects the stiffness is the orientation of anisotropic GDL to channels, which can affect not only the cell performance but also the durability

due to different stiffness and compressive distribution [66]. The perpendicular arrangement showed higher durability compared to the parallel arrangement, which was investigated through changes in the polarization curves, HFR, and MEA morphology showing detachment of the catalyst layer under the channel. Moreover, the GDL thickness likely affected the freeze/thaw durability; however, there was no discernable correlation between GDL

thickness and the durability [56,62] unless the thickness was closely related to the stiffness.

Along with the stiffness, the existence of an MPL can significantly affect the durability because it is a key layer in managing the water balance inside of a cell. The MPL is known to reduce mass transport loss by enhancing the water expulsion toward the channel. MPL eases the flooding of water and increases cell performance especially at high current density regions [68,69]. However, the MPL barely shows any positive influence on durability under freeze/thaw conditions. Kim et al. [56] concluded that the MPL does not mitigate the frost heave phenomenon, even if it restricts the intrusion of carbon fiber into the catalyst layer, as shown in SEM images. Furthermore, Lee et al. [70] inferred that the MPL yields more damage to the catalyst layer because it leaves more water in the membrane and the catalyst layer after the operation. This argument is supported by the cell performance and EIS data.

PTFE loading can also change the degradation mechanism. Lee et al. [71] investigated the effect of PTFE content on GDL, regarding its various properties such as porosity, bulk density, pore distribution, surface image, gas permeability, and contact angle. Because the PTFE physically covers the carbon fibers and binders, it suppresses the carbon fiber detachment and eases the structural changes, such as the formation of cracks on the MPL, at a cost of a decrease in porosity. However, the loss of PTFE occurs instead of carbon fibers or binders and causes a more rapid decrease in the contact angle.

Recently, the pore diameter and a hydrophilic layer in the GDL were also considered to affect cold start behavior [72,73]. The higher capillary pressure of a hydrophilic layer between the MPL and the substrate leads to absorbing more water from the catalyst layer to the hydrophilic layer; therefore, it inhibits the flooding in the catalyst and enhances cold start behavior from  $-10^{\circ}\text{C}$ , reducing the damage on the catalyst layer during the freeze/thaw process. The GDL with smaller pores showed less fluctuation in voltage and superior cold start-up performance at  $-5^{\circ}\text{C}$ . This is likely because the size of the water droplets is limited by the size of the pore and the smaller water droplets near the separator flow channel can be evaporated faster.

### 3.3. Dissolution effect on GDL

During the operation of a PEM fuel cell, the GDL is exposed to water or oxidative conditions. The GDL becomes hydrated by the water produced during the electrochemical reaction or supplied with hydrogen or oxygen gas. The accumulated water on the GDL can dissolve the GDL carbon material and generate hydroxide, oxides, and other species [74,75].

As some materials dissolve after a leaching test, the losses of the hydrophobicity and the weight of the GDL have been reported. Wood et al. [76] showed that the static contact angle decreased, especially during the first 100–200 h of the leaching test immersing a typical GDL substrate (Toray TGP-H containing 17 wt.% of fluorinated ethylene propylene (FEP)) in de-ionized (DI) water. In the paper by Frisk et al. [77], a weight loss of the micro-layer of up to 60% and a decrease in the contact angle from  $140^{\circ}$  to  $100^{\circ}$  were reported after being submerged in a bath of acidified 15 wt.% of hydrogen peroxide ( $\text{H}_2\text{O}_2$ ) solution. Latorrata et al. [78] conducted a leaching test by soaking GDL in a 20% sulfuric acid ( $\text{H}_2\text{SO}_4$ ) solution for 1000 h. After the accelerated test, the static contact angle of the substrate decreased from  $158.2 \pm 2^{\circ}$  to  $147 \pm 5^{\circ}$  and the total weight fell 3%. Noticeably, Ha et al. [79] showed the decreasing rate of the contact angle declined with test duration (Fig. 8). After 1000-h test, the contact angle reached a steady-state point because the materials that were vulnerable to the leaching effect had already been dissolved, and as a result, the contact angle was no longer affected by the leaching.

As factors that affect the dissolution of the GDL, MPL and PTFE have been the subject of debate due to their hydrophobic characteristics and both covering the GDL surface.

First, the effect of the MPL seems to be controversial. Fairweather et al. [80] exposed GDLs to PTFE-lined water baths filled with air-saturated water kept at  $80^{\circ}\text{C}$  and injected bubble air into DI water to maintain the conditions of the bath under oxidizing conditions. They showed that the MPL is influential for much slower changes of the contact angle not only on MPL itself but also on the fibrous substrate. With its granular structure, the MPL shields the fibers and restricts the contact of fibers with liquid

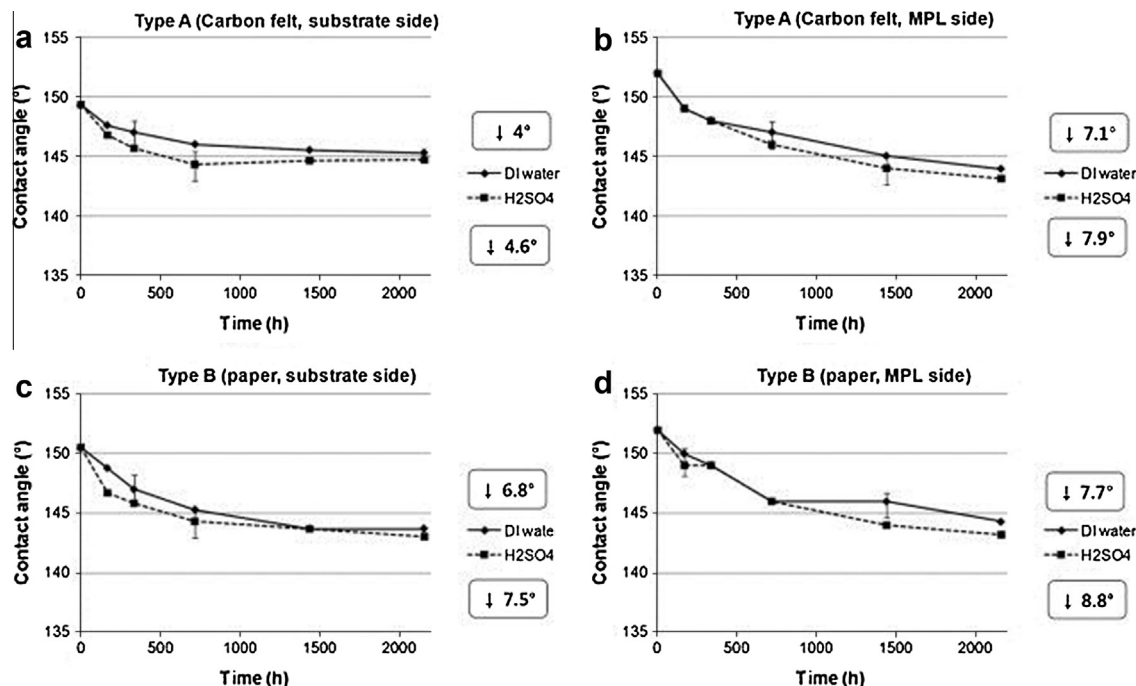


Fig. 8. The change of the static contact angle during leaching tests at (a) the substrate surface and (b) the MPL surface of a felt-type GDL, and at (c) the substrate surface and (d) the MPL surface of a paper-type GDL. (From [79] with permission.)



water because the MPL adhered to those fibers. However, Yu et al. [81] reported that the contact angle became considerably more acute in the MPL surface than the substrate surface by conducting the leaching test of 1200 h with  $\text{H}_2\text{SO}_4$ . Ha et al. [79] also showed that the change in the contact angle was greater on the MPL than the substrate after leaching tests of approximately 2000 h, as shown in Fig. 8.

In the aspect of PTFE, Fairweather et al. [80] concluded that there seemed to be no consistent difference according to the amount of PTFE. However, Das et al. [82] emphasized that higher content of PTFE is helpful in retarding the loss of hydrophobicity, which they investigated through the dynamic behavior of droplet relating to the water removal. The issue with PTFE loss during leaching tests has dissenting opinions. Larger holes, damage of PTFE coatings, and decreases in the structural integrity were observed through the series of field emission scanning electron microscope (FESEM) images in the paper by Yu et al. [81]. The author emphasized that infrared spectroscopy (IR) and thermal gravitational analysis (TGA) results indicate the detachment of PTFE coatings from the GDL, which is also supported by X-ray photoelectron spectroscopy (XPS) analysis. On the other hand, the paper by Ha et al. [79] confirmed that not PTFE but carbonized resin was lost during the leaching test, visualized through SEM images and TGA. These different analyses are initiated by the contradicting TGA results; therefore, more investigation on this subject is required.

Moreover, these material losses during leaching tests can affect GDL various properties and cell performance. A transient response of a PEM fuel cell after a leaching test of 2160 h in DI water was investigated by Cho et al. [83], as shown in Fig. 9. As the carbonized resin in a substrate decreases, a water lake can be easily formed in an aged GDL. This can interfere with the fuel supply toward the catalyst layer and reduce the hydration level of the membrane as it holds water rather than returns it to the membrane. Therefore, the aged GDL shows less voltage recovery after a sudden load change due to a low catalyst hydration capability. The authors showed it also displayed higher fluctuation of voltage due to uneven distribution of water and oxygen within the GDL. Yu et al. [81] conducted the leaching test of 1200 h with  $\text{H}_2\text{SO}_4$ , bringing about several changes in the physical properties, not only decreasing the contact angle and the damage of PTFE coatings but also creating larger holes, quadrupling the water permeability, and decreasing the structural integrity. The authors also emphasized that the irreversible structural changes altered the ratio of hydrophobic to hydrophilic surface area and negatively affected the transport of the reactants and a product. XPS analysis

supported their argument by showing that the atomic concentration of hydrophilic oxygen elements on the MPL surface increased from 0.22% to 2.13% while the concentration of hydrophobic fluorine elements changed from 47.02% to 30.60%, where the other percentage is occupied by carbon elements. The polarization curves indicated that the decrease in hydrophobicity results in poor cell performance even in low humidity conditions. This is because water could be transported more easily to the GDL, which causes membrane dehydration, resembling an analysis by Cho et al. [83]. In addition, the dissolution phenomenon deteriorates the mass transport capability. The loss of hydrophobicity mainly increased the cell performance at full load conditions [79], and the formation of large and deep cracks on the MPL surface increased the mass transfer resistance, as indicated by EIS and steady-state performance [78]. On the other hand, the change in the contact angle without any structural change barely affects the cell performance [84].

### 3.4. Erosion of GDL by continuous gas flow

As fuel gas flows between channels and the GDL, it can erode the layer. To mimic the erosion of GDL over its lifetime solely by gas flow effect, excessive air flow experiments were conducted by Ha [22] and Chun et al. [85]. To eliminate the degradation effect of electrochemical reactions, the catalyst layer was removed from the cell. Ha [22] inserted GDLs between a polycarbonate plate and a gas flow channel of the unit cell of  $330\text{ cm}^2$  with supplied air of 15 liters per minute (LPM). The 2400 h test found that the carbon paper-type GDL showed larger weight loss than the carbon felt-type GDL (paper-type:  $-1.1\%$ ; felt-type:  $-0.7\%$ ), while showing similar static contact angle loss of substrate from approximately  $147^\circ$  to approximately  $135^\circ$ . Chun et al. [85] accelerated the mechanical degradation by supplying a high flow rate of air (10 LPM) into the dummy cell of  $25\text{ cm}^2$ . Through 14 days of both dry and humidified gas experiments, they concluded that the damage on the surface of the MPL is mainly due to the water in the humidified air. The water gathers around the surface crack due to its lower local capillary pressure, and when the water is discharged from the MPL, the surface of the MPL is damaged, forming the puddle-shape defects shown in Fig. 10. Thus, the removal of surface crack on MPL may improve the durability of the GDL. Latorrata et al. [78] used the same dummy cell with air of 2 LPM on each side of a  $23\text{ cm}^2$  cell for over 1000 h. After the gas flow test, the contact angle of the substrate decreased from  $158.2 \pm 2^\circ$  to  $148 \pm 5^\circ$ , and the total weight of the GDL decreased to 80%. The gas flow also caused carbon erosion and detachment over large

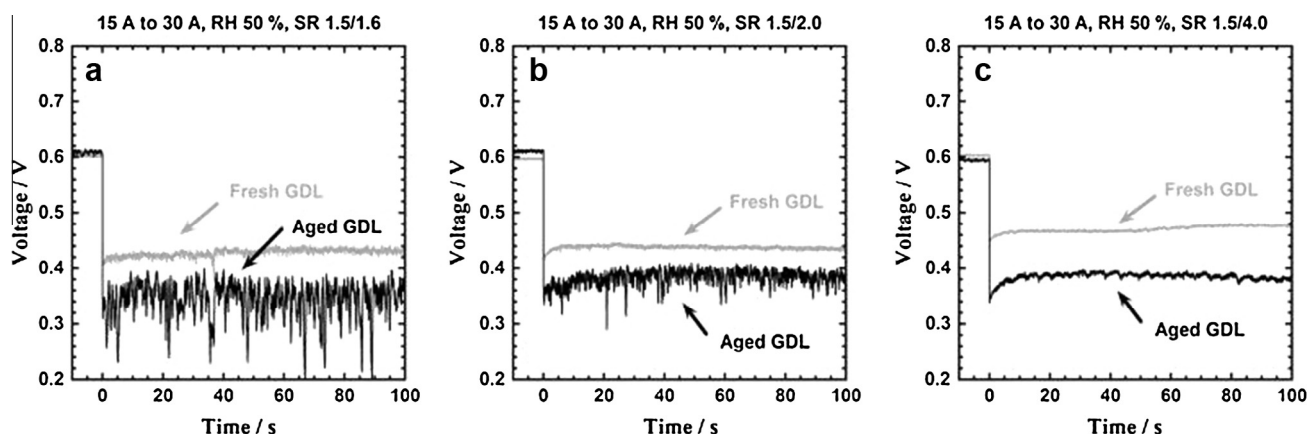


Fig. 9. The transient response of voltage as the current was changed from  $0.6\text{ A/cm}^2$  to  $1.2\text{ A/cm}^2$  at a relative humidity of 50% and a stoichiometric ratio of  $\text{H}_2/\text{air}$  of (a) 1.5/1.6 (starved), (b) 1.5/2.0 (standard), and (c) 1.5/4.0 (excess). (From [83] with permission.)



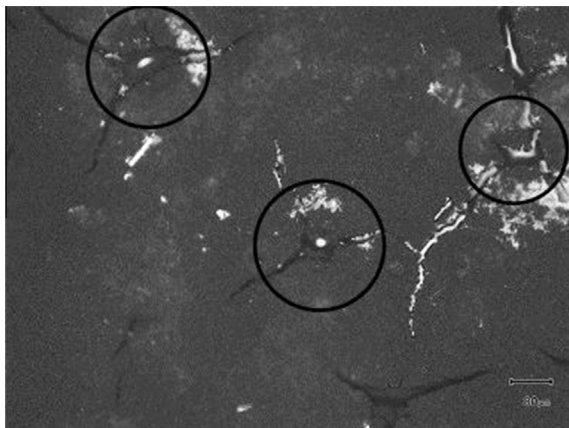


Fig. 10. Accumulation of water in puddle-shape defects and cracks (in circles) on the surface of degraded MPL. (From [85] with permission.)

part of the MPL and increased the mass transfer and ohmic resistances, as indicated through EIS and steady-state performance results.

#### 4. Chemical degradation on GDL

##### 4.1. Carbon corrosion phenomena of GDL

During the lifetime of the PEM fuel cell, it sometimes experiences carbon corrosion by electrical potential. The carbon corrosion can be explained by the decay mechanism related to local hydrogen starvation. During start/stop, shutdown, and localized hydrogen starvation conditions of the PEM fuel cell operation, air may be present on both the anode and cathode due to leakage and/or membrane crossover. Under these conditions, the supplied hydrogen can only occupy a portion of the anode, causing a high interfacial potential difference in the region where hydrogen is absent. The corresponding cathode region also has a high interfacial potential difference, which causes carbon corrosion and oxygen evolution at the cathode electrode. As shown in Fig. 11, reverse current causes the interfacial potential difference of the cathode to be 1.44 V [86]. Thus, under conditions over 1.44 V in the cell, carbon corrosion may occur and the durability of the cell is degraded, including the GDL.

The carbon corrosion process occurs in both the catalyst layer and the GDL. Because the GDL mainly consists of carbon fibers and carbon black, it is susceptible to structural damage from the corrosion. Frisk et al. [77] found that the corrosion current, which means the rate of oxidation, increases as the applied voltage to the GDL increases. Chen et al. [87] investigated the electrochemical durability of GDLs with an effective ex-situ method under simulated PEM fuel cell conditions. They conducted carbon corrosion tests with three-electrode cells. The GDLs were used as working electrodes, and a graphite board and a saturated calomel electrode were used as a counter electrode and a reference electrode, respectively. The prepared electrodes were held in a chamber filled with 0.5 M of  $\text{H}_2\text{SO}_4$  and maintained with a constant temperature of 80 °C. After 96 h of constant voltage at 1.0 V, 1.2 V, and 1.4 V (vs. SCE), the physical characteristics of the GDLs such as the surface profile, cross-sectional SEM image, and the surface contact angle were analyzed. The results showed that the in-plane resistivity and the through-plane permeability increased and the surface contact angle decreased as the oxidized potential increased. The cross-sectional SEM image (Fig. 12) showed that the inner layer was much more eroded than the outer layer. In addition, the number of macro-pores increased in the corroded GDLs. These corroded GDLs have a negative effect on the overall cell performance, especially in the high current density region. The reason for the performance deterioration is the increasing charge-transfer resistance and mass-transfer resistance. The EIS results showed that the charge-transfer and mass-transfer resistances of the fuel cell with the oxidized GDL with 1.2 V were approximately 40% and 22% larger than that of the cell with the fresh GDL, respectively. Ha et al. [88] introduced an accelerated carbon corrosion test of GDLs by applying 1.45 V with a power supply. They imitated the real operating fuel cell conditions by supplying hydrogen and air and maintaining the temperature of the cell when a 25 cm<sup>2</sup> unit fuel cell generates 1 A/cm<sup>2</sup>. The accelerated test was carried out for 96 h, which corresponds to five years of carbon corrosion in a fuel cell vehicle under maximum degradation conditions. By comparing the FESEM images of before and after the carbon corrosion test, they found that the thickness and the weight of GDL decreased. Through TGA analysis, they also discovered that the losses were mainly of the carbon materials, such as carbonized resin and carbon particles, not the PTFE coatings. In their paper, they concluded that the damage was done to the GDL internal structure and that the damage decreased the water removal ability of the GDL and impinged on the fuel cell performance. Yu et al. [89] also confirmed

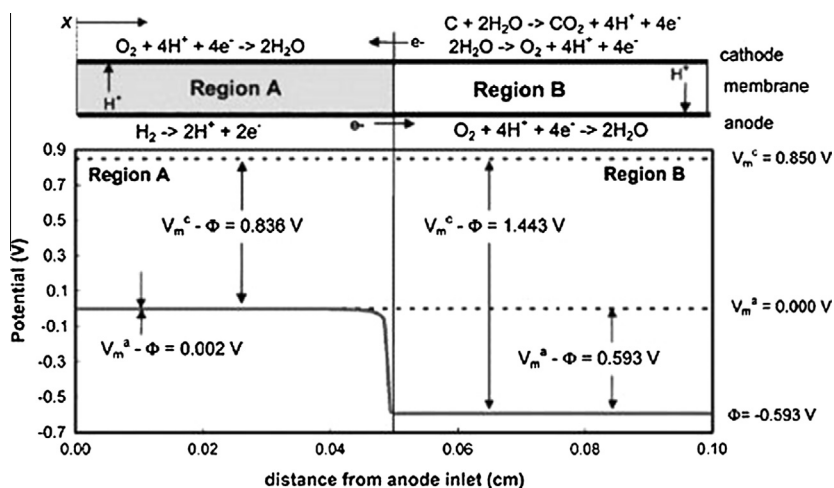
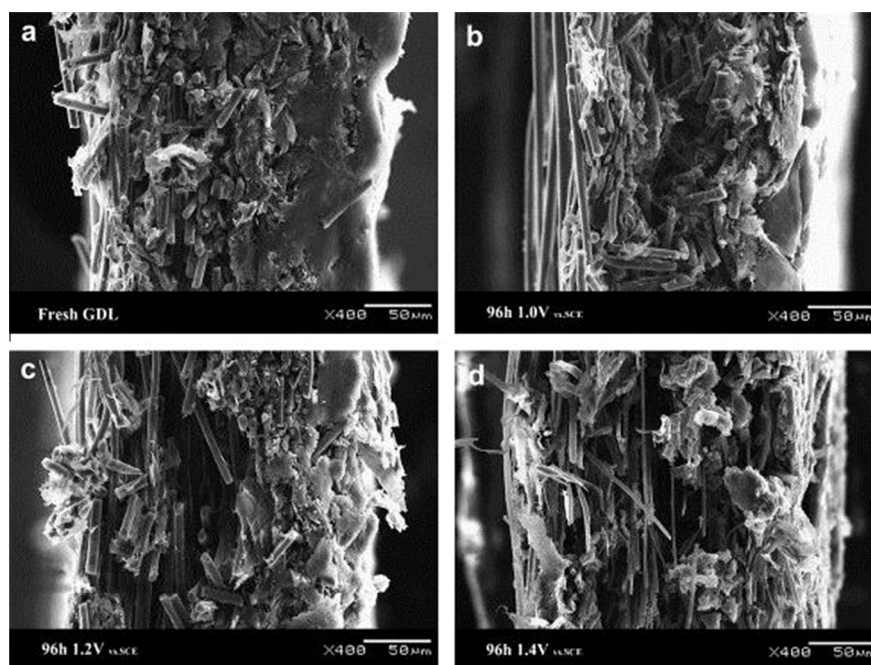


Fig. 11. Reverse decay mechanism of the PEM fuel cell. (Reprinted with permission from [86]. Copyright 2005, The Electrochemical Society.)



**Fig. 12.** The cross-sectional SEM images of (a) GDL before carbon corrosion and after 96 h carbon corrosion at: (b) 1.0 V, (c) 1.2 V, and (d) 1.4 V. (From [87] with permission.)

that the mass loss in GDL is mostly carbon material. However, they claimed that PTFE may be washed away as supporting carbon materials are washed away, hence decreasing the hydrophobicity of the GDL. Kumar et al. [90] explained the effect of electrochemical aging on carbon paper-type GDLs and carbon cloth-type GDLs. The GDL samples were aged in a three-electrode electrochemical cell with 0.5 M of  $\text{H}_2\text{SO}_4$  for 100 h. The GDL, platinum foil and standard calomel electrode were the working, counter and reference electrodes, respectively. The results indicated that a carbon paper-type GDL is more resistant to oxidation than a carbon cloth-type GDL. However, despite better oxidation resistance, the carbon paper-type GDL has less structural stability. Thus, after electrochemical aging, the structure of a carbon paper-type GDL is weakened so that the residual strain is increased when cyclic compression is applied to the GDL. Furthermore, the amount of GDL intruded to channel area was larger in the carbon paper-type GDL than the carbon cloth-type GDL.

Several papers examine the effect of MPL on the durability of the GDL. Spornjak et al. [91–93] compared cathode GDLs with and without an MPL by accelerated stress testing for carbon corrosion in a segmented PEM fuel cell under the condition of 1.3 V for 7 h. They quantified the carbon corrosion by measuring the  $\text{CO}_2$  evolution by a non-dispersive infrared sensor during the test. The results showed that the carbon corrosion of the catalyst layer was lower with the existence of MPL. The cell with MPL was observed to have lower kinetic losses, slower Pt particle growth, and higher active catalyst surface area. Thus, the performance degradation of a cell without MPL was more severe than a cell with MPL. Because MPL assists in the water discharge from catalyst to channel, the water content in the cell with MPL was lower, helping to mitigate the carbon corrosion at the catalyst layer. However, they mentioned that the mass transport is disadvantageous in a cell with MPL because the carbon corrosion is prone to occur at the boundary of the MPL, and other papers [87,88] observed the same phenomena. Consequently, MPL is advantageous in mitigating the carbon corrosion in the catalyst layer; however, the MPL itself is weak against carbon corrosion. Owejan et al. [94] identified the carbon corrosion in MPL through the use of a potential holding method at 1.2 V and accelerated startup/shutdown testing. They

conducted the carbon corrosion experiments using two types of GDLs: non-graphitized MPL and graphitized MPL. The result of the graphitized carbon in the MPL showed a 25% improvement of the voltage degradation rate at  $1.2 \text{ A/cm}^2$  compared to non-graphitized carbon in the MPL. These results showed that the graphitized carbon mitigates the carbon corrosion of the MPL and maintains its mass transport ability. Cho et al. [95] conducted an accelerated carbon corrosion stress test to determine the effect of MPL penetration on GDL degradation. Three samples with different MPL penetration thicknesses were used, and the results indicated that the GDL with the largest MPL penetration ratio (50%) showed better performance, especially in the high-load current density region, due to the enhanced water management caused by a balanced capillary pressure gradient inside of the GDL. However, the penetration region was observed to be more susceptible to corrosion due to the low binding force between the MPL and GDL substrate. These papers obviously show that the existence of MPL has a substantial impact on the carbon corrosion of GDL; hence, the material and the properties of the MPL are also significant parameters. Another important factor in the carbon corrosion of GDLs is the PTFE, along with the PTFE treatment. Perry et al. [96] conducted accelerated stress tests using air/air cycles. In each air/air cycle, the cell undergoes 1 h of exposure to air, followed by a 5 min supply of hydrogen with a nitrogen purge between each gas change (i.e., from air to hydrogen and back to air). The results showed that the performance decay rate was halved when the PTFE content in the MPL increased from 10% to 50%. Therefore, the PTFE in the MPL works as a resistance to oxidation. Kumar et al. [54] found that substrates treated with PTFE in multiple stages are advantageous for electrochemical durability. Though the GDL was loaded with the same amount of PTFE, the oxidation current decreased with increases in the number of stages of PTFE treatment. Furthermore, aged GDLs with PTFE loading stages of 1, 3, and 6 showed a decrease in the contact angle of 8%, 5%, and 3%, respectively.

In unutilized regenerative fuel cells, which can perform the water electrolytic cell, carbon corrosion on GDLs is inevitable as the cell operates with high positive potential in water electrolysis operation. Huang et al. [97] and Song et al. [98] used cycling tests of fuel

**Table A.1**  
Summary of durability tests in the literature.

Degradation condition	Approaches	Aging time	GDL types	Properties	Ref.
Compression force	Controlling GDL thickness by inserting steel gage	–	Felt	Permeability became one-tenth and in-plane and through-plane conductivity increased when the GDL was compressed to 65%	[41]
Compression force	Clamping method	–	Paper	Permeability became one-tenth and contact resistance decreased from 1000 to 25 mohm/cm <sup>2</sup> when the thickness was reduced by half	[42]
Compression force	Compression from 1.6 to 31.1 MPa	1 time	Cloth/ felt/paper	The thermal and contact resistances were lowered as the compression pressure increased	[43]
Compression force	Pressed with compressor	–	Cloth/paper	The contact resistance of cloth-type GDL was generally lower than that of the paper-based GDL	[44]
Compression force	Five-stack compression	–	Felt	The contact resistance and mass-transport resistance is in a trade-off relationship, with the contact resistance as the more dominant factor	[45]
Compression force	Compression at 100, 125, and 150 in-lb	1 time	Cloth/paper	The GDL porosity and contact resistance changed according to the clamping pressure	[46]
Compression force	Compression ratio from 10% to 45%	1 time	Cloth/paper	The paper-type GDL had large variations in the cell performance according to the clamping pressure compared to the cloth-type GDL	[47]
Compression force	Compression ratio varied with gasket thickness	–	Cloth	High areal weight GDL distributed force evenly and minimized the damage done by compression	[48]
Compression force	Compression from 0 to 10 MPa	2 times	Cloth/ felt/paper	The felt-type GDL had flexible and less brittle fibers before and after compression	[49]
Compression force	Compressed to 500 N/cm <sup>2</sup>	–	Felt/paper	The GDL was more resistant to compression when coated with MPL	[50]
Compression force	Pressed with compressor	–	Paper	Breakage of carbon fiber was observed when compressed 120 µm in thickness	[51]
Compression force	Repetitive compression under 1.7 and 3.4 MPa	5 times	Paper	Cyclic compression affects changes in the surface morphology, surface roughness, pore size, void fraction, and thickness	[52]
Compression force	Compression at 0.18, 0.36, 0.68, and 1.37 MPa	5 min	Paper	Irreversible damage was done at the surface of the fiber and PTFE coating breakage	[53]
Compression force/carbon corrosion	Cyclic compression under 3.4 MPa/3-electrode test under 1.2 V and 0.5 M of H <sub>2</sub> SO <sub>4</sub> at 80 °C	5 times/5 h	Paper	Multiple stages of PTFE loading is advantageous in durability under cyclic compression conditions	[54]
Compression force	Compression from 6.78–15.8 N	–	Felt/paper	More cross-over occurred in the felt-type GDL with rough MPL	[55]
Cold start	Cold start at –10, –20, and –40 °C	–	Cloth/paper	Performance decreased when the cell operated at low temperatures, and the decrease was more dominant in the paper GDL	[19]
Freeze/thaw cycle	Repetitive cycle from –35 °C to 20 °C	50 cycles	Paper	No change in the in-plane electrical resistivity, bending stiffness, surface contact angle, porosity, or water vapor diffusion were observed	[20]
Freeze/thaw cycle	Repetitive cycle from –40 °C to 70 °C	100 cycles	Cloth/paper	Higher stiffness of the GDL mitigated frost heave damage	[56]
Freeze/thaw cycle	Repetitive cycle from –20 °C to 10 °C	120 cycles	Felt	Severe void formation at the PEM/CCL interface, increased pore volume, and delamination of CCL were observed	[57]
Freeze/thaw cycle	Repetitive cycle from –40 °C to 70 °C	30 cycles	Felt	Non-crack catalyst with no GDL showed catastrophic layer delamination, while the GDL reduced the stress caused by the formation of ice and the damage to the catalyst layer	[58]
Freeze/thaw cycle	Repetitive cycle in both wet and dry conditions	120 (for dry)/62 (for wet) cycles	Paper	No significant structural changes of the GDL except for some cracks on the MPL surface	[59]
Freeze/thaw cycle	Repetitive cycle from –30 °C to 20 °C	10 cycles	Paper	Serious damage to the catalyst layer with severe cracks and segregation of the catalyst domain were observed	[60]
Freeze/thaw cycle	Repetitive cycle from –10 °C to 40 °C	50 cycles	Paper	Decreased maximum power density of –0.005% per cycle (cold purge), –0.07% per cycle (hot purge), and –0.1% per cycle (no purge)	[61]
Freeze/thaw cycle	Repetitive cycle from –40 °C to 70 °C	30/100 cycles	Cloth/ felt/paper	Greater degradation rate in flexible GDL from more free space for the ice formation, and little effect of the thickness and existence of the MPL layer	[62]
Freeze/thaw cycle	Repetitive cycle from –20 °C to 20 °C	20 cycles	Paper	Purging with a reactant gas with certain RH minimized the freezing damage while offering successful start-up	[63]
Freezing operation	Operating temperature between 0 and –15 °C	1 h	Unknown	The GDL surface became rougher due to the damage done in PTFE coating and binding particle with changing the gas permeability and electron conductivity	[64]
Freeze/thaw cycle	Repetitive cycle from –30 °C to 70 °C	50 cycles	Cloth/ felt/paper	The highly stiff felt GDL showed the best freeze/thaw durability, while cloth and paper GDLs had the medium and the worst durability, respectively	[65]
Freeze/thaw cycle	Repetitive cycle from –10 °C to 1 °C	1000 cycles	Felt	The GDL aligned perpendicular to the major flow field direction showed a higher durability than the GDL parallel to the flow field	[66]
Freeze/thaw cycle	Repetitive cycle from –40 °C to 80 °C	100 cycles	Cloth/paper	Deteriorated cell performance in carbon paper due to the breakage of fibers, decreased MPL contact angle, and detachment of catalyst was observed	[67]
Freeze/thaw cycle	Repetitive cycle from –15 °C to 70 °C	50 cycles	Felt/paper	The existence of MPL caused more damage to the catalyst layer due to more water remaining in the membrane	[70]

Table A.1 (continued)

Degradation condition	Approaches	Aging time	GDL types	Properties	Ref.
Freeze/thaw cycle	Repetitive cycle from $-20^{\circ}\text{C}$ to $10^{\circ}\text{C}$	10 times	Felt/paper	The reduction in the contact angle may be due to the separation of PTFE from the carbon fiber rather than the deformation of the planar pore structure	[71]
Cold start	Cold start test at $-5^{\circ}\text{C}$ and $-10^{\circ}\text{C}$	–	Paper	The hydrophilic layer between the MPL and the GDL improved the cell performance at subfreezing start-up conditions	[72]
Cold start	Cold start test at $-5^{\circ}\text{C}$ and $-10^{\circ}\text{C}$	–	Paper	Larger pore size showed higher limiting current density from a more open gas diffusion network, while smaller pore size showed anti-flooding behavior and remarkable cold start performance	[73]
Dissolution	Immersion in 30% $\text{H}_2\text{O}_2$ at $90^{\circ}\text{C}$ /cell operation at $80^{\circ}\text{C}$ & 0.6 V, 0.65 V, and 1.2 V	15 h/1111 h	Unknown	Carbon loss from GDLs and the catalyst layer is from both the carbon oxidation to carbon dioxide and the dissolution of partially oxidized graphene particle	[74]
Long-term operation	Cell temperature: $75^{\circ}\text{C}$ /humidifier temperature: $70^{\circ}\text{C}$ /stoichiometry ( $\text{H}_2/\text{air}$ ): 1/0.7, 1/0.4	6000 h	Refer to [75]	Carbon fiber oxidation caused the diffusion overvoltage to increase. The decrease in hydrophobicity due to the surface oxidation was negligible	[75]
Dissolution	Immersion in $60^{\circ}\text{C}$ or $80^{\circ}\text{C}$ of DI water with $\text{N}_2$ or air	700 h	Paper	The loss of EASA caused by aggregation or detaching or platinum particle should be minimized for improved durability	[76]
Dissolution/carbon corrosion	Immersion in 15% $\text{H}_2\text{SO}_4$ at $82^{\circ}\text{C}$ /carbon corrosion under 1.5 V	2000 h	Unknown	After 264 h, the current density dropped from $1\text{ A}/\text{cm}^2$ to $0.7\text{ A}/\text{cm}^2$ at 0.3 V due to the decreasing contact angle from $142^{\circ}$ to $102^{\circ}$	[77]
Erosion/dissolution	$23\text{ cm}^2$ dummy cell with 2 LPM air flow/immersion in 20% $\text{H}_2\text{SO}_4$	1000 h	Cloth	Erosion roughens the GDL surface, leading to worse contact. Chemical degradation creates deeper and larger cracks	[78]
Dissolution	Immersion in $80^{\circ}\text{C}$ of DI water and 10% $\text{H}_2\text{SO}_4$	2000 h	Paper/felt	Loss of hydrophobicity is due to the loss of carbonized resin instead of the loss of PTFE	[79]
Dissolution/carbon corrosion	Immersion in $80^{\circ}\text{C}$ of DI water/potential hold at 1, 1.2, and 1.5 V ( $\text{H}_2/\text{N}_2$ with 60, $80^{\circ}\text{C}$ )	200 h/1000 h	Paper	The contact angle decreased due to the formation of oxygen-containing groups	[80]
Dissolution	Immersion in 1 M $\text{H}_2\text{SO}_4$ for 72 h, then in a $70^{\circ}\text{C}$ water bath	1200 h	Unknown	Large holes appeared on the MPL surface and PTFE coating damage was observed on the substrate surface	[81]
Dissolution	Immersion in 30% $\text{H}_2\text{O}_2$ solution	7 h	Paper	Decreased contact angle as follows: No PTFE: $145^{\circ}$ to $141.5^{\circ}$ , 10% PTFE: $158^{\circ}$ to $155^{\circ}$ , 20% PTFE: $159^{\circ}$ to $155^{\circ}$ , 30% PTFE: $156.5^{\circ}$ to $152^{\circ}$	[82]
Dissolution	Immersion in $80^{\circ}\text{C}$ of DI water and 10% $\text{H}_2\text{SO}_4$	2000 h	Paper/felt	Locally, less hydrophobic areas formed a water lake and caused flooding	[83]
Dissolution/carbon corrosion	Immersion in $80^{\circ}\text{C}$ of 30% $\text{H}_2\text{O}_2$ solution/potential cycle from 0 to 1.5 V/long term cell operation	50 h/240 s/5000 h	Unknown	Wettability increased as the carbon surface oxidized, but had a minor effect on cell performance. Decreased diffusion at the catalyst layer and the GDL is the dominant factor for performance deterioration	[84]
Erosion	$330\text{ cm}^2$ dummy cell with 2 LPM air flow	2400 h	Felt/paper	The paper-type GDL showed heavier weight loss than the felt-type GDL while possessing similar static contact angle loss	[22]
Erosion	$25\text{ cm}^2$ dummy cell with 10 LPM air flow	28 days	Felt/paper	Puddle-shape defects swiftly formed around the crack, and water lingered around the defects, interfering with the reactant transport	[85]
Carbon corrosion	3-electrode test under 1.0, 1.2, and 1.4 V, 0.5 M of $\text{H}_2\text{SO}_4$ at $80^{\circ}\text{C}$	96 h	Paper	The maximum power densities decreased by 178 and $486\text{ mW}/\text{cm}^2$ when the GDLs were held at 1.2 and 1.4 V, respectively	[87]
Carbon corrosion	Cell holding at 1.45 V, $65^{\circ}\text{C}$ , RH 100%	96 h	Paper	The PTFE component of the GDL was not easily damaged by carbon corrosion, while carbon is easily damaged and removed	[88]
Carbon corrosion	3-electrode test at 1.25 V, 0.5 M of $\text{H}_2\text{SO}_4$	120 h	Unknown	The damage to the MPL morphologies increased the contact resistance	[89]
Compression force/carbon corrosion	Cyclic compression under 3.4 MPa/3-electrode test at 1.2 V, 0.5 M $\text{H}_2\text{SO}_4$ , $80^{\circ}\text{C}$	100 h	Cloth/paper	Carbon paper showed higher oxidation resistance compared to carbon cloth due to its graphitized carbon fibers	[90]
Dissolution/carbon corrosion	GDL boiling in 30% of $\text{H}_2\text{O}_2$ /potential hold at 1.3 V with $\text{H}_2/\text{N}_2$	5 min	Paper	Cell resistance is constant at the kinetic region but significantly increased at the mass transport region	[91]
Carbon corrosion	Potential hold at 1.3 V at $80^{\circ}\text{C}$ , RH 100%	7 h	Paper	The MPL mitigated electrochemical degradation because it discharged the produced water between the GDL and the catalyst layer	[92]
Carbon corrosion	Potential hold at 1.3 V ( $\text{H}_2/\text{N}_2$ , $80^{\circ}\text{C}$ ) for 3 h after potential hold at 1.2 V for 24 h	3 h	Paper	Degradation occurred in the MPL and then the catalyst layer	[93]
Carbon corrosion	Potential hold at 1.2 V and accelerated startup/shutdown testing under $\text{H}_2/\text{N}_2$	30 h	Paper	Graphitized carbon in the MPL mitigated the carbon corrosion and improved the cell performance	[94]
Dissolution/carbon corrosion	Immersion in 0.5 M of $\text{H}_2\text{SO}_4$ /3-electrode test at 1.45 V	96 h	Paper	MPL flooding occurred as the penetration area was eroded away, forming a water trap area	[95]
Carbon corrosion	Potential holding or cycling on a cell with air/air feed gas	310–620 h	Paper	Performance degradation by corrosion had a large impact when MPL was present, but an increase in the PTFE content alleviated the damage	[96]
Carbon corrosion	Potential cycle from 0 to 1.5 V	20 cycles	Paper	The corrosion of the MPL increased the contact resistance and severe water flooding	[97]
Carbon corrosion	Potential cycle from 0 to over 1.5 V	20 cycles	Paper	Cell performance decreased due to separation between the catalyst layer and membrane caused by evolution of hydrogen and oxygen	[98]



cell/water electrolytic cell mode with applying different constant voltages (i.e., 0.7 V for the fuel cell mode and 1.5 V for the water electrolytic cell mode) to investigate the corrosive effects on GDLs. Huang et al. [97] implied that the carbon corrosion occurred intensively on the MPL, which increased the contact resistance and induced water flooding. Song et al. [98] inferred that the carbon paper substrate was corroded by active oxygen species and the corrosion removed PTFE from the GDL. As corrosion-resistant GDLs, iridium-titanium nitride (Ir-TiN) based MPL and iridium dioxide coated titanium (IrO<sub>2</sub>/Ti) based MPL were suggested by Huang et al. [97] and Song et al. [98], respectively. Both samples showed higher durability than conventional carbon black of MPL.

## 5. Summary

According to various researchers, degradation of the GDL falls into two categorized degradation mechanisms: mechanical degradation and chemical degradation.

As the GDL is compressed, the thickness of the GDL decreases, leading to changes in both the electrical contact resistance and the gas permeability of the GDL. Better contact resistance enhances the ohmic overpotential, while lower gas permeability causes higher mass transport overpotential. Consequently, there is an optimum compression pressure of the GDL for enhancing the fuel cell performance.

The GDL is also degraded under freeze/thaw conditions. The stiffness of the GDL is the most important factor for the GDL durability under freeze/thaw conditions. Thus, the durability of the GDL under freeze/thaw conditions is affected by the GDL type. In addition, the amount of PTFE and the existence of MPL also affect the durability of the GDL.

Some GDL materials can be dissolved when the GDL is exposed to water or oxidative conditions, causing loss of weight and hydrophobicity of the GDL. Decreases in the contact angle mean that the hydrophobicity of the GDL is lowered, which results in a poor water management ability of the GDL and degradation of the fuel cell performance.

Another stressor of the mechanical degradation is the erosion effect. As the reactant and product gases flow between the channel and the GDL, the GDL surface is eroded, especially concentrated on the surface crack. Furthermore, the contact angle and the weight of the GDL also decrease when the GDL is exposed to continuous gas flow.

Carbon corrosion is the representative stressor of the chemical degradation of the GDL. The carbon materials of the GDL are oxidized and the durability of the GDL is lowered under the carbon corrosion condition. The carbon corrosion in the GDL is affected by the existence of the MPL and mitigated by the amount of PTFE loading and corrosion-resistant treatment.

To date, the durability research on GDL is relatively limited, even though GDLs are very important among the PEM fuel cell components. From the literature, degraded GDLs show that material loss and changes in the structure, resulting in degradation of fuel cell performance due to lower water management and mass transport.

Degradation of the cell components is an interactive process that occurs simultaneously. Therefore, understanding the degradation mechanism of a stand-alone GDL and studying the contribution of each stressor of the GDL degradation over the fuel cell lifetime are necessary. Furthermore, standardized test protocols need to be established to evaluate GDL durability. Then, implementing a mitigation strategy for GDL degradation and investigating the effect of GDL durability on other PEM fuel cell components will be possible. Finally, further studies on the GDL durability will expand the lifetimes of fuel cell vehicles and stationary systems and promote the commercialization of PEM fuel cell applications.

## Acknowledgments

This work was supported by the New & Renewable Energy Core Technology Program of the Korea Institute of Energy Technology Evaluation and Planning (KETEP), granted financial resource from the Ministry of Trade, Industry & Energy, Republic of Korea (No. 20143010031880), Brain Korea 21 (BK21) PLUS, and SNU Institute of Advanced Machines and Design (IAMD).

## Appendix A

The detailed summary of durability tests in the literature is shown in Table A.1. It contains the information of degradation condition, approach, aging time, GDL type, and property change.

## References

- [1] Recent Climate Change: Atmosphere Changes. EPA; 2007.
- [2] Russell R. The Greenhouse Effect & Greenhouse Gases. University Corporation for Atmospheric Research Windows to the Universe; 2007.
- [3] Staudt A, Huddleston N, Rudenstein S. Understanding and responding to climate change. The National Academy of Sciences; 2007: 14.
- [4] Mundial B. World Development Report 2010: Development and Climate Change. World Bank; 2010.
- [5] Emissions, Reducing Transport Greenhouse Gas: Trends and Data 2010. International transport forum: OECD; 2010. p. 94.
- [6] Chen J, Matsuura T, Hori M. Novel gas diffusion layer with water management function for PEMFC. *J Power Sources* 2004;131:155–61.
- [7] Li H, Tang Y, Wang Z, Shi Z, Wu S, Song D, et al. A review of water flooding issues in the proton exchange membrane fuel cell. *J Power Sources* 2008;178:103–17.
- [8] Yousfi-Steiner N, Moçotéguy P, Candusso D, Hissel D, Hernandez A, Aslanides A. A review on PEM voltage degradation associated with water management: Impacts, influent factors and characterization. *J Power Sources* 2008;183:260–74.
- [9] Cao T-F, Lin H, Chen L, He Y-L, Tao W-Q. Numerical investigation of the coupled water and thermal management in PEM fuel cell. *Appl Energy* 2013;112:1115–25.
- [10] Hosseinzadeh E, Rokni M, Rabbani A, Mortensen HH. Thermal and water management of low temperature Proton Exchange Membrane Fuel Cell in fork-lift truck power system. *Appl Energy* 2013;104:434–44.
- [11] Park S-K, Choe S-Y, Lim T-W, Kim J-S, Seo D-H, Choi J. Analysis of a shell-and-tube type gas-to-gas membrane humidifier for an automotive polymer electrolyte membrane fuel cell power system. *Int J Automot Technol* 2013;14:449–57.
- [12] Cho J, Oh H, Park J, Min K, Lee E, Jyoung J-Y. Effect of the micro porous layer design on the dynamic performance of a proton exchange membrane fuel cell. *Int J Hydrogen Energy* 2014;39:459–68.
- [13] Cho J, Oh H, Park J, Min K, Lee E, Jyoung J-Y. Study on the performance of a proton exchange membrane fuel cell related to the structure design of a gas diffusion layer substrate. *Int J Hydrogen Energy* 2014;39:495–504.
- [14] Guo H, Liu X, Zhao JF, Ye F, Ma CF. Experimental study of two-phase flow in a proton exchange membrane fuel cell in short-term microgravity condition. *Appl Energy* 2014;136:509–18.
- [15] Pei P, Chen H. Main factors affecting the lifetime of Proton Exchange Membrane fuel cells in vehicle applications: a review. *Appl Energy* 2014;125:60–75.
- [16] Cho J. Study on transient response characteristics of a PEM fuel cell related with structure and degradation effects of a gas diffusion layer: Seoul National University; 2012.
- [17] Park J. Study on the effects of structural characteristics of gas diffusion layer on water management and cell performance with PEM fuel cell model: Seoul National University; 2015.
- [18] Garland N, Benjamin T, Kopasz J. DOE fuel cell program: durability technical targets and testing protocols. *ECS Trans* 2007;11:923–31.
- [19] Mukundan R, Lujan R, Davey JR, Spendlow JS, Hussey DS, Jacobson DL, et al. Ice formation in PEM fuel cells operated isothermally at sub-freezing temperatures. *ECS Trans* 2009;25:345–55.
- [20] Lee C, Merida W. Gas diffusion layer durability under steady-state and freezing conditions. *J Power Sources* 2007;164:141–53.
- [21] Martin J, Wu J, Wang H. Ballard-NRC IFCI joint research project on gas diffusion layer accelerated stress testing. IFCI technical report; 2007.
- [22] Ha T. Analysis of degradation characteristics in gas diffusion layer of PEM Fuel Cell: Seoul National University; 2010.
- [23] Yuan X-Z, Li H, Zhang S, Martin J, Wang H. A review of polymer electrolyte membrane fuel cell durability test protocols. *J Power Sources* 2011;196:9107–16.
- [24] Mench MM, Kumbur EC, Veziroglu TN. Polymer electrolyte fuel cell degradation. Academic Press; 2011.

- [25] Zhang S, Yuan X-Z, Hin JNC, Wang H, Friedrich KA, Schulze M. A review of platinum-based catalyst layer degradation in proton exchange membrane fuel cells. *J Power Sources* 2009;194:588–600.
- [26] Zhang S, Yuan X, Wang H, Mérida W, Zhu H, Shen J, et al. A review of accelerated stress tests of MEA durability in PEM fuel cells. *Int J Hydrogen Energy* 2009;34:388–404.
- [27] Yousfi-Steiner N, Mocotéguy P, Candusso D, Hissel D. A review on polymer electrolyte membrane fuel cell catalyst degradation and starvation issues: causes, consequences and diagnostic for mitigation. *J Power Sources* 2009;194:130–45.
- [28] Büchi FN, Inaba M, Schmidt TJ. Polymer electrolyte fuel cell durability. Springer; 2009.
- [29] Wu J, Yuan XZ, Martin JJ, Wang H, Zhang J, Shen J, et al. A review of PEM fuel cell durability: degradation mechanisms and mitigation strategies. *J Power Sources* 2008;184:104–19.
- [30] Schmittinger W, Vahidi A. A review of the main parameters influencing long-term performance and durability of PEM fuel cells. *J Power Sources* 2008;180:1–14.
- [31] De Bruijn F, Dam V, Janssen G. Review: durability and degradation issues of PEM fuel cell components. *Fuel Cells* 2008;8:3–22.
- [32] Borup R, Meyers J, Pivovar B, Kim YS, Mukundan R, Garland N, et al. Scientific aspects of polymer electrolyte fuel cell durability and degradation. *Chem Rev* 2007;107:3904–51.
- [33] Borup R, Davey J, Wood D, Garzon F, Inbody M, Guidry D. PEM fuel cell durability. FY: DOE hydrogen program; 2005.
- [34] Liu W, Ruth K, Rusch G. The membrane durability in PEM fuel cells. *J New Mater Electrochem Syst* 2001;4:227–32.
- [35] Shao Y, Yin G, Wang Z, Gao Y. Proton exchange membrane fuel cell from low temperature to high temperature: material challenges. *J Power Sources* 2007;167:235–42.
- [36] Peighambarioust S, Rowshanzamir S, Amjadi M. Review of the proton exchange membranes for fuel cell applications. *Int J Hydrogen Energy* 2010;35:9349–84.
- [37] Knights SD, Colbow KM, St-Pierre J, Wilkinson DP. Aging mechanisms and lifetime of PEFC and DMFC. *J Power Sources* 2004;127:127–34.
- [38] Wang Y, Chen KS, Mishler J, Cho SC, Adroher XC. A review of polymer electrolyte membrane fuel cells: technology, applications, and needs on fundamental research. *Appl Energy* 2011;88:981–1007.
- [39] Borup RL, Davey JR, Garzon FH, Wood DL, Inbody MA. PEM fuel cell electrocatalyst durability measurements. *J Power Sources* 2006;163:76–81.
- [40] 2014 Journal Citation Reports® (Thomson Reuters; 2014).
- [41] Nitta I, Hottinen T, Himanen O, Mikkola M. Inhomogeneous compression of PEMFC gas diffusion layer Part I. Exp *J Power Sources* 2007;171:26–36.
- [42] Chang WR, Hwang JJ, Weng FB, Chan SH. Effect of clamping pressure on the performance of a PEM fuel cell. *J Power Sources* 2007;166:149–54.
- [43] Ihonen J, Mikkola M, Lindbergh G. Flooding of gas diffusion backing in PEFCs – physical and electrochemical characterization. *J Electrochem Soc* 2004;151:A1152–61.
- [44] Mishra V, Yang F, Pitchumani R. Measurement and prediction of electrical contact resistance between gas diffusion layers and bipolar plate for applications to PEM fuel cells. *J Fuel Cell Sci Tech* 2004;1:2–9.
- [45] Yim SD, Kim BJ, Sohn YJ, Yoon YG, Park GG, Lee WY, et al. The influence of stack clamping pressure on the performance of PEM fuel cell stack. *Curr Appl Phys* 2010;10:S59–61.
- [46] Lee WK, Ho CH, Van Zee JW, Murthy M. The effects of compression and gas diffusion layers on the performance of a PEM fuel cell. *J Power Sources* 1999;84:45–51.
- [47] Ge JB, Higier A, Liu HT. Effect of gas diffusion layer compression on PEM fuel cell performance. *J Power Sources* 2006;159:922–7.
- [48] Lin JH, Chen WH, Su YJ, Ko TH. Effect of gas diffusion layer compression on the performance in a proton exchange membrane fuel cell. *Fuel* 2008;87:2420–4.
- [49] Escribano S, Blachot J-F, Ethève J, Morin A, Mosdale R. Characterization of PEMFCs gas diffusion layers properties. *J Power Sources* 2006;156:8–13.
- [50] Wilde PM, Maendle M, Murata M, Berg N. Structural and physical properties of GDL and GDL/BPP combinations and their influence on PEMFC performance. *Fuel Cells* 2004;4:180–4.
- [51] Matsuura T, Kato M, Hori M. Study on metallic bipolar plate for proton exchange membrane fuel cell. *J Power Sources* 2006;161:74–8.
- [52] Radhakrishnan V, Haridoss P. Effect of cyclic compression on structure and properties of a Gas Diffusion Layer used in PEM fuel cells. *Int J Hydrogen Energy* 2010;35:11107–18.
- [53] Bazylak A, Sinton D, Liu ZS, Djilali N. Effect of compression on liquid water transport and microstructure of PEMFC gas diffusion layers. *J Power Sources* 2007;163:784–92.
- [54] Kumar RJF, Radhakrishnan V, Haridoss P. Enhanced mechanical and electrochemical durability of multistage PTFE treated gas diffusion layers for proton exchange membrane fuel cells. *Int J Hydrogen Energy* 2012;37:10830–5.
- [55] Baik KD, Kim SI, Hong BK, Han K, Kim MS. Effects of gas diffusion layer structure on the open circuit voltage and hydrogen crossover of polymer electrolyte membrane fuel cells. *Int J Hydrogen Energy* 2011;36:9916–25.
- [56] Kim S, Chacko C, Ramasamy RP, Mench MM. Freeze-induced damage and purge based mitigation in polymer electrolyte fuel cells. *ECS Trans* 2007;11:577–86.
- [57] Lee SY, Kim HJ, Cho E, Lee KS, Lim TH, Hwang IC, et al. Performance degradation and microstructure changes in freeze-thaw cycling for PEMFC MEAs with various initial microstructures. *Int J Hydrogen Energy* 2010;35:12888–96.
- [58] Kim S, Mench MM. Physical degradation of membrane electrode assemblies undergoing freeze/thaw cycling: micro-structure effects. *J Power Sources* 2007;174:206–20.
- [59] Alink R, Gerteisen D, Suipok M. Degradation effects in polymer electrolyte membrane fuel cell stacks by sub-zero operation – an in situ and ex situ analysis. *J Power Sources* 2008;182:175–87.
- [60] Guo QH, Qi ZG. Effect of freeze-thaw cycles on the properties and performance of membrane-electrode assemblies. *J Power Sources* 2006;160:1269–74.
- [61] Luo MJ, Huang CY, Liu W, Luo ZP, Pan M. Degradation behaviors of polymer electrolyte membrane fuel cell under freeze/thaw cycles. *Int J Hydrogen Energy* 2010;35:2986–93.
- [62] Kim S, Ahn BK, Mench MM. Physical degradation of membrane electrode assemblies undergoing freeze/thaw cycling: diffusion media effects. *J Power Sources* 2008;179:140–6.
- [63] Hou JB, Yu HM, Zhang SS, Sun SC, Wang HW, Yi BL, et al. Analysis of PEMFC freeze degradation at -20 degrees C after gas purging. *J Power Sources* 2006;162:513–20.
- [64] Yan QG, Toghiani H, Lee YW, Liang KW, Causey H. Effect of sub-freezing temperatures on a PEM fuel cell performance, startup and fuel cell components. *J Power Sources* 2006;160:1242–50.
- [65] Lim SJ, Park GG, Park JS, Sohn YJ, Yim SD, Yang TH, et al. Investigation of freeze/thaw durability in polymer electrolyte fuel cells. *Int J Hydrogen Energy* 2010;35:13111–7.
- [66] Han K, Hong BK, Kim SH, Ahn BK, Lim TW. Influence of anisotropic bending stiffness of gas diffusion layers on the degradation behavior of polymer electrolyte membrane fuel cells under freezing conditions. *Int J Hydrogen Energy* 2011;36:12452–64.
- [67] Mukundan R, Kim YS, Rockward T, Davey JR, Pivovar B, Hussey DS, et al. Performance of PEM fuel cells at sub-freezing temperatures. *ECS Trans* 2007;11:543–52.
- [68] Kim T, Lee S, Park H. A study of water transport as a function of the microporous layer arrangement in PEMFCs. *Int J Hydrogen Energy* 2010;35:8631–43.
- [69] Kitahara T, Konomi T, Nakajima H. Microporous layer coated gas diffusion layers for enhanced performance of polymer electrolyte fuel cells. *J Power Sources* 2010;195:2202–11.
- [70] Lee Y, Kim B, Kim Y, Li XG. Effects of a microporous layer on the performance degradation of proton exchange membrane fuel cells through repetitive freezing. *J Power Sources* 2011;196:1940–7.
- [71] Lee Y, Kim B, Kim Y, Li XG. Degradation of gas diffusion layers through repetitive freezing. *Appl Energy* 2011;88:5111–9.
- [72] Hirakata S, Hara M, Kakinuma K, Uchida M, Tryk DA, Uchida H, et al. Investigation of the effect of a hydrophilic layer in the gas diffusion layer of a polymer electrolyte membrane fuel cell on the cell performance and cold start behaviour. *Electrochim Acta* 2014;120:240–7.
- [73] Hirakata S, Mochizuki T, Uchida M, Uchida H, Watanabe M. Investigation of the effect of pore diameter of gas diffusion layers on cold start behavior and cell performance of polymer electrolyte membrane fuel cells. *Electrochim Acta* 2013;108:304–12.
- [74] Chlistunoff J, Davey JR, Rau KC, Mukundan R, Borup RL. PEMFC Gas Diffusion Media Degradation Determined by Acid-Base Titrations. *ECS Trans* 2013;50:521–9.
- [75] Hiramitsu Y, Sato H, Kobayashi K, Honi M. Controlling gas diffusion layer oxidation by homogeneous hydrophobic coating for polymer electrolyte fuel cells. *J Power Sources* 2011;196:5453–69.
- [76] David Wood JX, Susan Pacheco, John Davey, Rod Borup. Durability issues of the PEMFC GDL and MEA under steady-state and drive-cycle operating conditions; 2004.
- [77] Frisk J, Hicks M, Atanasoski R, Boand W, Schmoedel A, Kurkowski M. MEA component durability. 3M Company, St. Paul, MN; 2004.
- [78] Latorrata S, Stampino PG, Cristiani C, Dotelli G. Novel Superhydrophobic Gas Diffusion Media for PEM Fuel Cells: Evaluation of Performance and Durability. *CHEMICAL ENGINEERING*; 2014: 41.
- [79] Ha T, Cho J, Park J, Min K, Kim HS, Lee E, et al. Experimental study of the effect of dissolution on the gas diffusion layer in polymer electrolyte membrane fuel cells. *Int J Hydrogen Energy* 2011;36:12427–35.
- [80] Fairweather JD, Li B, Mukundan R, Fenton J, Borup RL. In situ and ex situ characterization of carbon corrosion in PEMFCs. *ECS Trans* 2010;33:433–46.
- [81] Yu SC, Li XJ, Li J, Liu S, Lu WT, Shao ZG, et al. Study on hydrophobicity degradation of gas diffusion layer in proton exchange membrane fuel cells. *Energy Convers Manage* 2013;76:301–6.
- [82] Das PK, Grippin A, Kwong A, Weber AZ. Liquid-water-droplet adhesion-force measurements on fresh and aged fuel-cell gas-diffusion layers. *J Electrochem Soc* 2012;159:B489–96.
- [83] Cho J, Ha T, Park J, Kim HS, Min K, Lee E, et al. Analysis of transient response of a unit proton-exchange membrane fuel cell with a degraded gas diffusion layer. *Int J Hydrogen Energy* 2011;36:6090–8.
- [84] Aoki T, Matsunaga A, Ogami Y, Maekawa A, Mitsushima S, Ota K, et al. The influence of polymer electrolyte fuel cell cathode degradation on the electrode polarization. *J Power Sources* 2010;195:2182–8.
- [85] Chun JH, Jo DH, Kim SG, Park SH, Lee CH, Kim SH. Improvement of the mechanical durability of micro porous layer in a proton exchange membrane fuel cell by elimination of surface cracks. *Renew Energy* 2012;48:35–41.

- [86] Reiser CA, Bregoli L, Patterson TW, Jung SY, Yang JD, Perry ML, et al. A reverse-current decay mechanism for fuel cells. *Electrochem Solid-State Lett* 2005;8:A273–6.
- [87] Chen GB, Zhang HM, Ma HP, Zhong HX. Electrochemical durability of gas diffusion layer under simulated proton exchange membrane fuel cell conditions. *Int J Hydrogen Energy* 2009;34:8185–92.
- [88] Ha T, Cho J, Park J, Min K, Kim HS, Lee E, et al. Experimental study on carbon corrosion of the gas diffusion layer in polymer electrolyte membrane fuel cells. *Int J Hydrogen Energy* 2011;36:12436–43.
- [89] Yu SC, Li XJ, Liu S, Hao JK, Shao ZG, Yi BL. Study on hydrophobicity loss of the gas diffusion layer in PEMFCs by electrochemical oxidation. *Rsc Adv* 2014;4:3852–6.
- [90] Kumar RJF, Radhakrishnan V, Haridoss P. Effect of electrochemical aging on the interaction between gas diffusion layers and the flow field in a proton exchange membrane fuel cell. *Int J Hydrogen Energy* 2011;36:7207–11.
- [91] Spornjak D, Fairweather JD, Rockward T, Rau KC, Spendelow JS, Borup RL, et al. Influence of in situ and ex situ aging of gas diffusion layers on fuel cell performance degradation. Conference. In: ECS Meeting, Honolulu; 2012. p. 16721678.
- [92] Spornjak D, Fairweather J, Mukundan R, Rockward T, Borup RL. Influence of the microporous layer on carbon corrosion in the catalyst layer of a polymer electrolyte membrane fuel cell. *J Power Sources* 2012;214:386–98.
- [93] Spornjak D, Fairweather JD, Rockward T, Mukundan R, Borup R. Characterization of Carbon Corrosion in a Segmented PEM Fuel Cell. *ECS Trans* 2011;41:741–50.
- [94] Owejan JE, Paul TY, Makharia R. Mitigation of carbon corrosion in microporous layers in PEM fuel cells. *ECS Trans* 2007;11:1049–57.
- [95] Cho J, Park J, Oh H, Min K, Lee E, Jyoung JY. Analysis of the transient response and durability characteristics of a proton exchange membrane fuel cell with different micro-porous layer penetration thicknesses. *Appl Energy* 2013;111:300–9.
- [96] Perry ML, Patterson T, Madden T. GDL degradation in PEFC. *ECS Trans* 2010;33:1081–7.
- [97] Huang SY, Ganesan P, Jung HY, Popov BN. Development of supported bifunctional oxygen electrocatalysts and corrosion-resistant gas diffusion layer for unitized regenerative fuel cell applications. *J Power Sources* 2012;198:23–9.
- [98] Song SD, Zhang HM, Ma XP, Shao ZG, Zhang YN, Yi BL. Bifunctional oxygen electrode with corrosion-resistant gas diffusion layer for unitized regenerative fuel cell. *Electrochem Commun* 2006;8:399–405.